The protein encoded by the US3 orthologue of Marek's disease virus is required for efficient de-envelopment of perinuclear virions and involved in actin stress fiber breakdown

Daniel Schumacher, B Karsten Tischer, Sascha Trapp, Nikolaus Osterrieder

JOURNAL OF VIROLOGY, Apr. 2005, p. 3987–3997 Vol. 79, No. 7
0022-538X/05/$08.00+0 doi:10.1128/JVI.79.7.3987–3997.2005

The Protein Encoded by the U_S3 Orthologue of Marek's Disease Virus Is Required for Efficient De-Envelopment of Perinuclear Virions and Involved in Actin Stress Fiber Breakdown

Daniel Schumacher, B. Karsten Tischer, Sascha Trapp, and Nikolaus Osterrieder*

Department of Microbiology and Immunology, College of Veterinary Medicine, Cornell University, Ithaca, New York

Received 18 August 2004/Accepted 10 November 2004

Marek's disease virus (MDV) encodes a protein exhibiting high amino acid similarity to the U_S3 protein of herpes simplex virus type 1 and the gene 66 product of varicella-zoster virus. The MDV U_S3 orthologue was replaced with a kanamycin resistance gene in the infectious bacterial artificial chromosome clone BAC20. After transfection of U_S3-negative BAC20 DNA (20ΔU_S3), the resulting recombinant 20ΔU_S3 virus exhibited markedly reduced growth kinetics. Virus titers on chicken embryo cells were reduced by approximately 10-fold, and plaque sizes were significantly smaller (65% reduction) compared to parental BAC20 virus. The defect of the U_S3-negative MDV was completely restored in a revertant virus (20U_S3*) expressing a U_S3 protein with a carboxy-terminal FLAG tag. Electron microscopical studies revealed that the defect of the 20ΔU_S3 mutant to efficiently spread from cell to cell was concomitant with an accumulation in the perinuclear space of primarily enveloped virions in characteristic vesicles containing several virus particles, which resulted in reduced numbers of particles in the cytoplasm. The formation of these vesicles was not observed in cells infected with either parental BAC20 virus or the 20U_S3* revertant virus. The role of the MDV U_S3 protein in actin stress fiber breakdown was investigated by visualizing actin with phalloidin-Alexa 488 after infection or transfection of a U_S3 expression plasmid. Addition of the actin-depolymerizing drug cytochalasin D to cells transfected or infected with BAC20 resulted in complete inhibition of plaque formation with as little as 50 nM of the drug, while concentrations of nocodazole as high as 50 μM only had a relatively minor effect on MDV plaque formation. The results indicated that the MDV U_S3 serine-threonine protein kinase is transiently involved in MDV-mediated stress fiber breakdown and that polymerization of actin, but not microtubules, plays an important role in MDV cell-to-cell spread.

Marek's disease (MD) is a highly contagious lymphoproliferative disease of chickens caused by the cell-associated Marek's disease virus (MDV). MDV (gallid herpesvirus 2 [GaHV-2]) is currently classified within the recently established genus *Mardivirus* ("Marek's disease-like viruses") within the *Alphaherpesvirinae* subfamily. The *Mardivirus* genus is formed by MDV and its close relatives, GaHV-3, which was previously referred to as MDV-2, and the herpesvirus of turkeys (HVT). Only MDV, but not GaHV-3 or HVT, can cause MD (6, 7, 28). The complete genome sequences of MDV, GaHV-3, and HVT are available, and the MDV genome is approximately 177 kbp in length, encoding at least 103 proteins (43). MD caused by oncogenic MDV can successfully be prevented by vaccination with the genetically and antigenically closely related and nonpathogenic GaHV-3 and HVT, or by using attenuated MDV strains (33, 45, 46).

Currently, knowledge on the essential or nonessential nature of individual MDV genes or the functions of its encoded proteins in the virus' life cycle is very limited. Only in 2000 was it possible to isolate the first MDV mutant harboring a deletion of an essential gene, when open reading frame (ORF) U_L27 encoding glycoprotein B (gB) was deleted from the genome. The gB-negative mutant virus was constructed from an infectious bacterial artificial chromosome (BAC) clone of avirulent MDV strain 584Ap80C by the insertion of a kanamycin resistance cassette in lieu of the gB gene (39). Since the description of the MDV gB mutant, five other ORFs (U_L10 encoding gM, U_L49 encoding VP22, $U_L49.5$ encoding gM's complex partner, U_S7 encoding gI, and U_S8 encoding gE) have also been described to be essential for replication of MDV in cell culture (10, 40, 42).

It is generally accepted that the early stages of MDV replication are identical to those described for the prototype member of the *Alphaherpesvirinae*, herpes simplex virus type 1 (HSV-1) (34). After entry of a virus capsid into an uninfected cell, nucleocapsids travel to the nuclear pore, where the viral genome is released and translocated into the nucleus. The genome is replicated and subsequently packaged into preformed capsids. The assembled nucleocapsid then acquires a primary envelope by budding at the inner leaflet of the nuclear membrane and is present in the perinuclear space in the endoplasmic reticulum (ER). In a following de-envelopment step, virions then lose their primary envelope by an as-of-yet-poorly understood fusion with the outer leaflet of the nuclear membrane. As a result of this de-envelopment step, naked nucleocapsids are released into the cytoplasm, where they obtain their final envelope during a secondary and final envelopment step, which takes place at cytoplasmic vesicles that likely are derived from the *trans*-Golgi network or endosomes (15).

Several HSV-1 proteins were shown to be involved in the primary envelopment and the following de-envelopment at the inner and outer nuclear membrane, among them the products

* Corresponding author. Mailing address: Department of Microbiology & Immunology, College of Veterinary Medicine, Cornell University, Ithaca, NY 14853. Phone: (607) 253-4045. Fax: (607) 253-3384. E-mail: no34@cornell.edu.

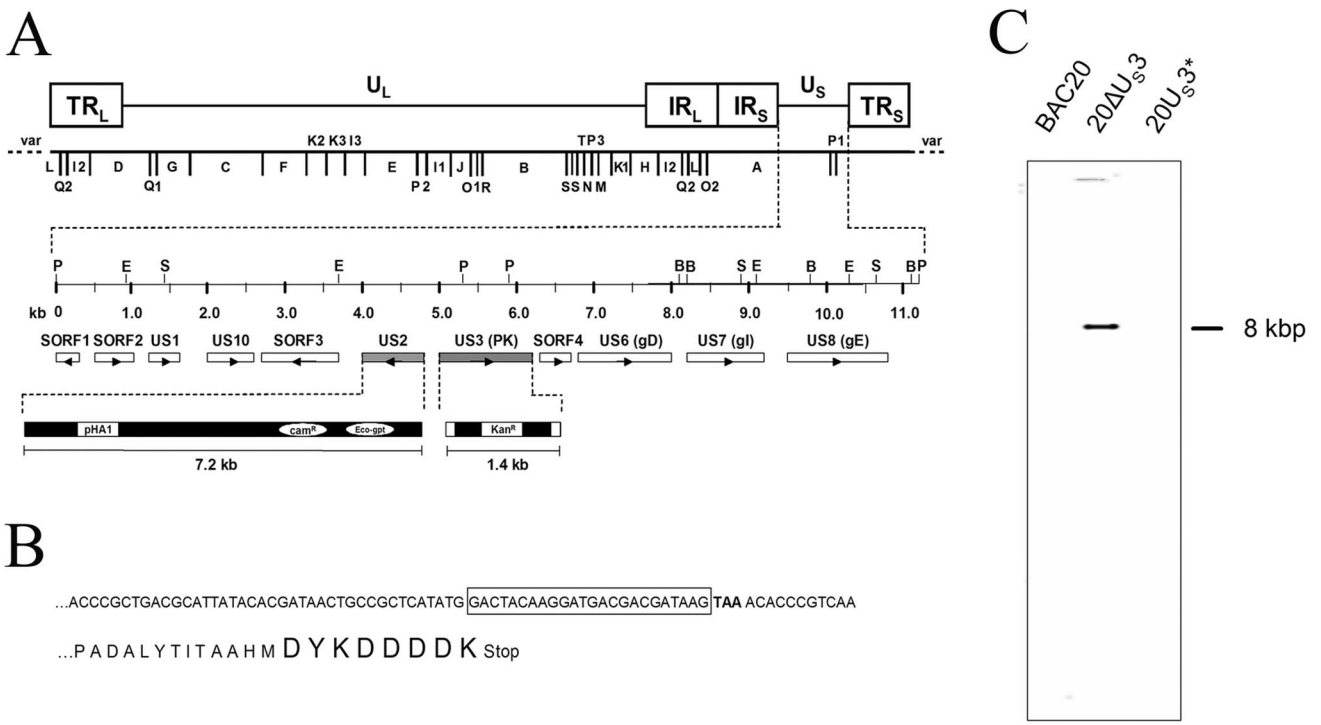

FIG. 1. (A) Schematic illustration of the procedure to delete the U_S3 ORF from BAC20. Shown is the organization of the approximately 185-kbp BAC20 genome and the BamHI restriction map. The unique short region (U_S) with the introduced pHA1 sequence as well as the introduced *kan*^{r} gene is highlighted. (B) The construction of the rescuant viruses, harboring a FLAG tag at the carboxy terminus of the U_S3, is shown. Small letters indicate original amino acid sequences, while large letters denote the introduced FLAG tag. (C) Digitally scanned image of a Southern blot. DNA from BAC20, 20ΔU_S3, and 20U_S3* was cleaved with BamHI and transferred to a nylon membrane. The blot was incubated with a digoxigenin-labeled *kan*^{r}-specific probe. Specific hybridization was detected by chemiluminescence using CSPD (Roche Biochemicals).

of U_L11, U_L31, U_L34, U_L53 (gK), and U_S3. The function of the U_L11 product on the early stages of HSV-1 egress is unclear. While the pseudorabies virus (PRV) and equine herpesvirus type 1 homologues appear to act in a later step of virus morphogenesis in the cytoplasm (18, 38), an HSV-1 U_L11 mutant virus was characterized by an accumulation of nucleocapsids in the nucleus, juxtaposed to the inner lamella of the nuclear membrane. In addition, the number of particles in the cytoplasm was increased (1, 22). Recently, the U_L16 product has been shown to serve as a binding partner for U_L11 (23). gK—besides its function in entry and suppression of extensive membrane fusion in later stages of infection—is necessary for primary envelopment of newly synthesized nucleocapsids in nondividing cells (11-13, 16).

Studies on the products of the U_L31 and U_L34 genes have shown that these proteins form a complex that is localized at the nuclear rim and is essential for primary envelopment of nucleocapsids (31, 47). The U_L34 product (pU_L34), which also is a substrate for the HSV-1 U_S3-encoded kinase, represents a type II transmembrane protein, and its long N terminus protrudes into the cyto- and nucleoplasm while the short carboxy terminus resides in the ER. The N-terminal domain of pU_L34 interacts with another viral protein, pU_L31, which is involved in disintegration of the nuclear lamins, thereby presumably facilitating access of newly formed nucleocapsids to the nuclear membrane. Although it has been shown that pU_S3 phosphorylates pU_L34, phosphorylation of pU_L34 is not required for even distribution and that of its complex partner pU_L31 along the nuclear rim. However, it has been shown that the nuclear rim distribution of both pU_L34 and pU_L31 are dependent—at least in some cell types—on the kinase activity of pU_S3, indicating that phosphorylation of yet another protein is required (35). Deletion of the U_S3 gene in both HSV-1 and PRV caused an accumulation of virus particles between the two leaflets of the nuclear envelope and eventually resulted in reduced virus titers (17, 30, 32, 35). Besides the role pU_S3 plays in shuttling of virions out of the ER, it also appears to confer resistance to apoptosis and mediate actin stress fiber breakdown (21, 26, 44).

In this report, we aimed at elucidating the different roles that the U_S3 protein plays in MDV infection. We constructed a mutant virus carrying a deletion in the U_S3 gene from the well-characterized BAC20 clone (39). Our experiments show that a virus lacking the MDV protein kinase encoded by U_S3 has a growth defect in cultured cells that is concomitant with an accumulation of primarily enveloped virus particles in the perinuclear space. In addition, we were able to demonstrate that the MDV U_S3 protein is involved in the rearrangement of the cytoskeleton in infected cells by virus-induced actin stress fiber breakdown.

MATERIALS AND METHODS

Virus and cells. Chicken embryo cells (CEC) were prepared from 11-day-old chicken embryos and maintained at 37°C under a 5% CO_2 atmosphere in minimal essential medium supplemented with 1 to 10% fetal bovine serum. MDV BAC20 virus (20) was recovered after transfection of BAC20 DNA (39). Transfections of mutant BAC clones, expression plasmid pcU_S3* that harbors the FLAG epitope at the carboxy terminus of the U_S3 ORF (Fig. 1) and expression

plasmid pcMgB, harboring MDV-1 gB (39), was performed accordingly using 1 to 5 μg of BAC or plasmid DNA. In some experiments, CEC transfected with BAC20 DNA or infected with BAC20 virus were incubated in the presence of various concentrations of cytochalasin D or nocodazole (Sigma) in the cell culture medium. Media were changed every 12 h. At various times after infection or transfection, cells were fixed; plaques and single infected cells were stained by indirect immunofluorescence (IIF) and counted.

Plasmids and PCR. PCR amplification of the fragment containing the kanamycin resistance (*kan*^{r}) gene that was used for Red mutagenesis was obtained by using plasmid pKD13 (5) as a template. The primers U_S3-for (5′-AATCTTATACTCTGGTAGAATATGAAACAGGGTTAAAACTAGGTAATAGA**CGTGTAGGCTGGAGCTGCTTC**-3′) and U_S3-rev (5′-CGCGTAGTATATATTATAAAATGAATCATTGAAGTTATTTTTGACGGGTG**CATTCCGGGGATCCGTCGAC**-3′) contained 20 nucleotides each of *kan*^{r}-specific sequences (bold letters) and 50 nucleotides of MDV-specific sequences to allow homologous recombination with the viral sequences and the deletion of the U_S3 gene. The PCR product was then used for production of U_S3-negative BAC20 exactly as previously described (40) (Fig. 1). The MDV U_S3 ORF was amplified from strain 584Ap80C by standard PCR. A carboxy-terminally FLAG-tagged version of pU_S3 was created by introduction of the FLAG epitope (DYKDDDDK) immediately in front of the stop codon (Fig. 1). The entire U_S3 ORF, without the stop codon but including an additional 1,000 bp upstream of U_S3, was PCR amplified using a sense primer, U_S3-FLAG-1 (5′-GACCACGTTTTAGTCTACGT-3′), and an antisense primer, U_S3-FLAG-2 (5′-CTTATCGTCGTCATCCTTGTAGTCCATATGAGCGGCAGTTATCG-3′). In a second PCR with primers U_S3-FLAG-3 (5′-GACTACAAGGATGACGACGATAAGTAAACACCCGTCAAAAATAA-3′) and U_S3-FLAG-4 (5′-ATAACAGTTATAGGAGACGC-3′), the U_S3 stop codon and an additional 700 bp downstream of U_S3 were amplified. The products of both PCRs served as templates in a third PCR, in which the primers U_S3-FLAG-1 and U_S3-FLAG-4 were used to amplify the entire FLAG-tagged U_S3 ORF and the flanking sequences. Additionally, the complete FLAG-tagged U_S3 ORF was amplified using primers U_S3*amp1 (5′-TAATAGACTGGATGTCTTCG-3′) and U_S3*amp2 (5′-TTACTTATCGTCGTCATCCTTG-3′) and cloned into the pcDNA3.1/V5-His TOPO vector (Invitrogen). The generated plasmid was named pcU_S3*.

Mutagenesis of BAC20 and generation of rescuant virus. Mutagenesis of BAC20 DNA was performed using *Escherichia coli* EL250 cells, which inducibly express the λ phage recombination enzymes Exo, Beta, and Gam (20). Electrocompetent EL250 cells carrying BAC20 were prepared after induction of expression of Exo, Beta, and Gam by a temperature shift to 42°C and further incubation for 15 min (25). Three hundred nanograms of a purified PCR product designed to delete the target sequences (Fig. 1) was electroporated into 40 μl of electrocompetent BAC20-containing cells under standard electroporation conditions (1.25 kV/cm, 200 Ω, 25 μF). After electroporation, cells were grown in 1 ml of Luria-Bertani broth for 60 min at 32°C and plated onto Luria-Bertani agar plates containing 30 μg of chloramphenicol/ml and 30 μg of kanamycin/ml. Double-resistant colonies were isolated and further analyzed (37). Large-scale preparations of mutant BAC DNAs were done using a commercially available kit (QIAGEN).

Rescuant $20U_S3$* virus expressing the FLAG epitope was recovered by cotransfecting CEC with $20\Delta U_S3$ DNA and the PCR product, in which the FLAG tag was introduced at the carboxy terminus of U_S3 (see above) (Fig. 1). Single plaques were isolated and grown in parallel plates, one of which was checked for expression of the FLAG-tagged U_S3 protein by standard IIF using the monoclonal anti-FLAG M2 antibody (Stratagene) at a 1:500 dilution (see below).

DNA analyses. BAC DNA was cleaved with restriction endonucleases (NEB, Fermentas) and separated on 0.8% agarose gels. DNA fragments were transferred to positively charged nylon membranes (Pharmacia-Amersham), and Southern blot hybridization was performed using a digoxigenin-labeled *kan*^{r} probe. Chemoluminescent detection of DNA-DNA hybrids using CSPD was done according to the supplier's instructions (Roche Biochemicals) (40).

Virus growth kinetics and plaque area determinations. Virus growth kinetics were determined after infection of 10^6 CEC with 150 PFU of the different viruses. At various times after infection, infected cells were trypsinized and titers were determined by plating the infected cells onto fresh CEC in serial 10-fold dilutions. Plaque areas were measured after plating of the viruses on CEC and 5 days of incubation at 37°C. Cells were fixed and analyzed by IIF with MDV gB-specific monoclonal antibody (MAb) 2K11 (9). For each virus, 100 plaques were measured by taking digital pictures of individual plaques and measuring the plaque area using the documentation software ImageJ (http://rsb.info.nih.gov/ij/index.html). Average percentages of plaque areas and standard deviations were determined from at least three independent experiments. Where indicated, statistical analyses were performed with SAS version 8.2 for Windows (SAS Institute).

Western blotting, IIF, and confocal laser-scanning microscopy (CLSM). For Western blot analyses, CEC lysates were prepared at 4 days after infection. Samples were separated by sodium dodecyl sulfate (SDS)–10% polyacrylamide gel electrophoresis (PAGE) and transferred to nitrocellulose membranes (Schleicher & Schüll) by the semidry method (19). After blocking, blots were incubated with anti-FLAG MAb M2 at a 1:10,000 dilution or with anti-VP22 MAb L13 (1:100 dilution) (9). Bound antibodies were detected with an anti-mouse immunoglobulin G (IgG)–peroxidase conjugate (Sigma) and visualized by enhanced chemiluminescence (Pharmacia-Amersham) using X-ray films (Amersham Biosciences).

IIF was done exactly as described previously (40). Infected or transfected cells grown on glass coverslips were fixed with 90% acetone. Free binding sites were blocked with phosphate-buffered saline–10% fetal bovine serum, and anti-gB MAb 2K11, anti-VP5 MAb 3F19, or an MDV-specific chicken serum was added for 30 min. After two washing steps in phosphate-buffered saline-Tween, Alexa 488- or Alexa 568-conjugated anti-mouse or anti-chicken IgG antibodies were added for 30 min. Polymerized actin was detected by staining with 1 U of AlexaFluor 488 phalloidin (Molecular Probes), and microtubules were visualized with a Cy3-conjugated anti-β-tubulin MAb (Sigma). After two final washing steps, cells were inspected. Coverslips were mounted onto glass slides using Fluoromount-G (Southern Biotechnology Associates, Inc.) and viewed by conventional fluorescence microscopy (Zeiss Axiovert 25) or CLSM using an Olympus Fluoview 500. Green and red fluorescence signals were recorded separately using appropriate filters for excitation and detection exactly as described previously (27). IIF and confocal images were processed using Adobe Photoshop 7.0.

Electron microscopy. Three days after inoculation, uninfected or infected cells in T75 cell culture flasks (Costar) were fixed for 30 min with 2.5% glutaraldehyde buffered in 0.1 M Na-cacodylate (300 mosM; pH 7.4). After washing with 0.1 M Na-cacodylate, cells were scraped off of the plate, pelleted by low-speed centrifugation, postfixed in 1.0% aqueous OsO_4 (Electron Microscopy Science), and finally stained with uranyl acetate. After stepwise dehydration in ethanol, cells were embedded in epon araldite (Electron Microscopy Science) and polymerized at 60°C for 1 day. Ultrathin sections of embedded material were counterstained with uranyl acetate and lead salts and examined in an electron microscope (Philips EM 400Tecnai).

RESULTS

Characterization of a U_S3-negative MDV mutant. To investigate the function of the MDV U_S3 gene product, a mutant ($20\Delta U_S3$) was constructed that lacked the entire ORF. A linear PCR fragment encoding the *kan*^{r} gene and 50 bp of flanking sequences up- and downstream of the U_S3 gene to allow homologous recombination into the targeted sequence was electroporated into EL250 cells harboring BAC20. Individual kanamycin and chloramphenicol double-resistant colonies harboring modified BAC clones were picked. One of the colonies was chosen for further analysis and termed $20\Delta U_S3$. Extrachromosomal BAC DNA was prepared, cleaved with BamHI, and separated by 0.8% agarose gel electrophoresis. BamHI-cleaved DNA showed the alterations in the restriction enzyme pattern that were predicted after insertion of the *kan*^{r} gene into the BAC20 sequence. A 9.8-kbp fragment present in BAC20 DNA was absent in $20\Delta U_S3$. Instead, an 8.0-kbp and a 1.9-kbp fragment appeared. The genotype of $20\Delta U_S3$ was confirmed by Southern blot analysis using a *kan*^{r}-specific probe. As expected, the probe only hybridized to the modified 8.0-kbp fragment present in mutant $20\Delta U_S3$ DNA (Fig. 1C). Sequencing of the junctions between the resistance gene and viral DNA sequences in the chosen clone proved the correct insertion of the antibiotic resistance gene and the absence of the U_S3 gene (data not shown).

Growth characteristics of $20\Delta U_S3$ and rescuant $20U_S3$* virus. The replication of $20\Delta U_S3$ virus was tested in cultured CEC and compared to that of parental BAC20 and revertant $20U_S3$* virus, which expresses a FLAG-tagged version of the unique-short protein kinase, named pU_S3*. BAC DNA was

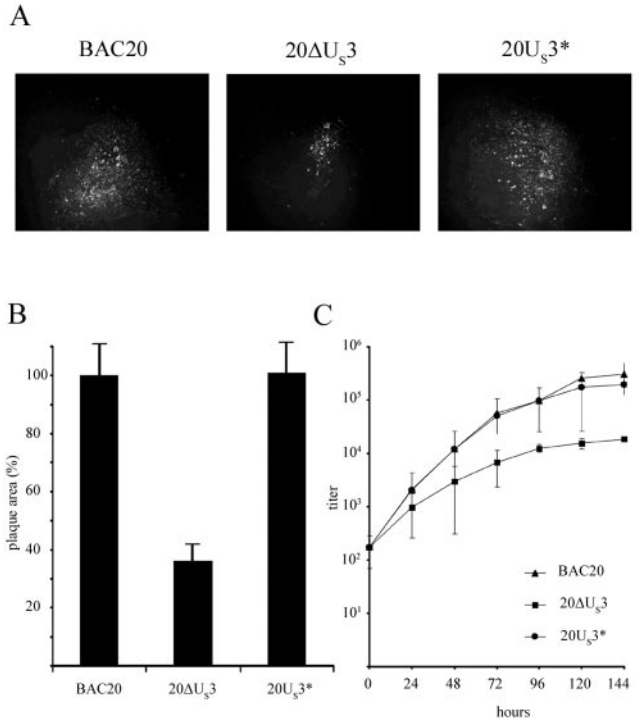

FIG. 2. (A) CEC were infected with BAC20, 20ΔU_S3, or 20U_S3* and fixed with 90% acetone at 5 days p.i. Plaques were analyzed by IIF using anti-gB MAb 2K11. Bound antibodies were detected anti-mouse IgG Alexa 488 (Molecular Probes). (B) For each virus, digital pictures of at least 100 plaques were taken and plaque sizes were measured. The mean plaque area of BAC20 virus was set to 100%, and average relative plaque areas of the 20ΔU_S3 and 20U_S3* viruses were calculated. Standard deviations are also given. Plaque areas and standard deviations were determined from three independent experiments. (C) Growth properties of BAC20, 20ΔU_S3, and 20U_S3* viruses recovered after transfection of BAC DNA. A total of 10^6 CEC were infected with 150 PFU of the respective virus. At the given times p.i., cells were trypsinized, titrated, and coseeded with fresh CEC. Virus plaques were counted after IIF staining with MAb 2K11. Mean virus titers and standard deviations of the results of three independent experiments are shown.

transfected into primary CEC, and virus growth was monitored. Compared to the parental virus, growth of reconstituted 20ΔU_S3 was markedly reduced. Whereas MDV-specific plaques were visible from day 3 after transfection of parental BAC20 DNA, virus plaques after transfection of 20ΔU_S3 DNA could not be observed until day 5 after transfection. When plaque sizes of both viruses were determined at 5 days postinfection (p.i.), a significant difference between parental virus and 20ΔU_S3 was observed (Fig. 2A and B). The sizes of 20ΔU_S3-induced plaques were reduced by more than 65% compared to parental BAC20 plaques (Fig. 2B). To further analyze the growth defect of the 20ΔU_S3 mutant, virus growth kinetics were performed. This assay also revealed a marked reduction in the ability of the 20ΔU_S3 mutant virus to replicate in cultured chicken cells (Fig. 2C), and maximum titers of 20ΔU_S3 in CEC were reduced by approximately 10-fold compared to those of the BAC20 virus.

In order to confirm that the observed reductions in plaque sizes and titers of the 20ΔU_S3 mutant were indeed attributable to the deletion of the ORF and not to spurious mutations elsewhere in the viral genome, a rescuant virus was constructed in which the kanamycin resistance gene was replaced by a U_S3 ORF that was PCR amplified from BAC20. To detect rescuant virus after cotransfection and to facilitate protein detection, the FLAG epitope was added to the extreme carboxy-terminal end of the U_S3 protein (Fig. 1B). Rescuant virus was isolated by cotransfection of the mutant BAC clone and a PCR product encompassing the previously introduced deletion. After cotransfection of 20ΔU_S3 DNA and the PCR product containing the FLAG-tagged U_S3 gene, recombinant virus plaques were readily detectable because their sizes were significantly larger than those in which the U_S3 gene was not expressed (Fig. 2A). Plaque purification and IIF analysis of the obtained rescuant virus confirmed the successful insertion of the modified U_S3 gene into the negative mutant virus (data not shown).

After amplification of the rescuant 20U_S3* virus, plaque sizes and virus growth kinetics were determined. Both 20U_S3* plaque sizes and growth kinetics were virtually identical to those of parental BAC20 virus and were significantly increased compared to those of the U_S3-negative mutant virus (Fig. 2B and C). From the results of these assays, we concluded that the rescuant 20U_S3* revertant virus was virtually indistinguishable from parental BAC20 with respect to the growth characteristics in cultured cells and that the observed growth defects of the 20ΔU_S3 mutant were not caused by fortuitous mutations outside of the U_S3 ORF.

To analyze and monitor expression of the FLAG-tagged pU_S3* in infected cells, Western blot analyses were performed using the anti-FLAG M2 antibody (Stratagene). CEC were infected with BAC20, 20ΔU_S3, or 20U_S3* virus. At day 4 p.i., cells were harvested and lysed and infected cell proteins were adjusted to equal protein concentrations before separation by SDS–10% PAGE. The FLAG-specific M2 antibody reacted with a protein of an approximate M_r of 48,000 in lysates of cells infected with 20U_S3*. This band was not visible in lysates of mock-infected

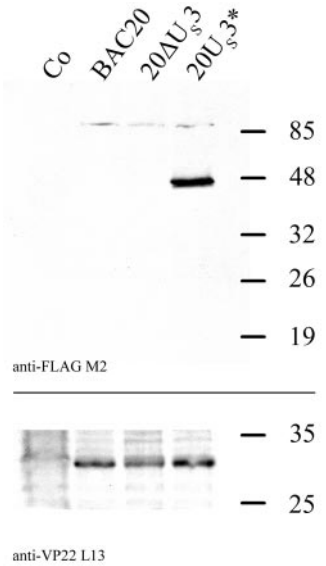

FIG. 3. Western blot analysis of CEC infected with BAC20, 20ΔU_S3, and 20U_S3*. Cells were harvested and lysed at 4 days p.i. Cell lysates were separated by SDS–10% PAGE and transferred to nitrocellulose. Identical blots were incubated with either anti-FLAG MAb M2 or anti-VP22 MAb L13. The molecular weights of a molecular weight marker (Fermentas) are given in thousands. Co, mock-infected CEC.

TABLE 1. Percentages of virus particles in cellular compartments

Virus	% Intranuclear	% Perinuclear space	% Cytoplasm	Total particles/cells counted
BAC20	75	1	24	248/38
$20\Delta U_S3$	61	35	4	180/21
$20U_S3$*	65	2	33	343/26

cells or cells infected with BAC20 or $20\Delta U_S3$ virus (Fig. 3). The absence of the M_r 48,000 band in lysates of cells infected with BAC20 or $20\Delta U_S3$ virus was not caused by an absence of virus infection, since a control reaction with the anti-VP22 MAb L13 confirmed comparable levels of infection and viral protein synthesis in all lysates of virus-infected cells (Fig. 3).

The absence of MDV pU_S3 results in accumulation of enveloped virions in the perinuclear space. To investigate the role of the U_S3 protein during virus replication in more detail, CEC were infected with the various viruses and examined by transmission electron microscopy at 3 days p.i. Cells infected with $20\Delta U_S3$ showed normal de novo morphogenesis of nucleocapsids in the nucleus, and the numbers of A, B, and C capsids were comparable to those observed in the case of BAC20 virus-infected cells. However, in the absence of pU_S3, enveloped virions accumulated in the perinuclear space (Fig. 4A). Clusters of up to 15 newly formed and primarily budded virions appeared to be stalled in protrusions bordered by the inner and outer leaflet of the nuclear membrane. No such accumulations and aggregations of virus particles were observed in cells infected with the parental BAC20 (data not shown) or the $20U_S3$* virus (Fig. 4B). All stages of virion maturation were observed, including nucleocapsid formation in infected cell nuclei, primary budding at the inner leaflet of the nuclear membrane, primarily enveloped viruses in the perinuclear space, naked nucleocapsids in the cytoplasm, secondary budding at cytoplasmic vesicles, and the presence of mature virions in transport vesicles (Fig. 4B). Since the same stages of virus morphogenesis were observed after infection and analysis of CEC infected with BAC20 or $20U_S3$* virus, the observed defect was indeed caused by the absence of pU_S3 in the $20\Delta U_S3$ mutant virus. Quantifications of newly synthesized virus particles in different cellular compartments were also conducted. While particle numbers in the nuclei of cells infected with BAC20 virus, the U_S3-negative virus, or the revertant virus were very similar (Table 1), numbers of particles between the inner and outer leaflet of the nuclear membrane were largely increased in cells infected with $20\Delta U_S3$ virus compared to cells infected with parental or revertant virus (Table 1). In contrast, the number of virus particles in the cytoplasm was reduced in the absence of the U_S3 protein and only reached approximately 12 to 16% of the particle counts determined for cells infected with either BAC20 or the $20U_S3$* virus (Table 1). From the results of the transmission electron microscopical analyses, we concluded that the accumulation of virus particles in the perinuclear space is probably caused by a defect in fusion of primarily enveloped virions with the outer leaflet of the nuclear membrane and that this defect causes an accumulation of virions in the perinuclear space that is accompanied by decreased particle numbers in the cytoplasm. The defect in de-envelopment and reduced cytoplasmic particle counts might at least partially explain the reduced plaque sizes and virus titers of $20\Delta U_S3$ in vitro.

MDV pU_S3 induces a transient actin stress fiber breakdown in transfected cells. Functional studies on the PRV U_S3 protein had shown that actin stress fiber breakdown can be mediated by the unique-short protein kinase. To determine the possible effects of MDV pU_S3 on the cytoskeleton, CEC were either infected with BAC20, $20\Delta U_S3$, and $20U_S3$* virus or transfected with expression plasmid pcU_S3*.

Owing to the high cell association of MDV that requires the coseeding of infected with uninfected cells for virus propagation and amplification, synchronous and/or high-multiplicity infections of CEC could not be performed. As a consequence, quantification of the number of infected cells that exhibited a disassembly of actin stress fibers or of the time point after infection at which disassembly started was very difficult. In three independent experiments, MDV infection was monitored by IIF staining with a convalescent chicken serum, while actin filaments were visualized using phalloidin-Alexa 488. It could be shown that actin stress fiber disassembly was more common in cells infected with either the parental BAC20 or the revertant $20U_S3$* virus than with the $20\Delta U_S3$ virus. After infection with BAC20 or $20U_S3$* virus, cells with at least partially intact actin stress fibers could clearly be observed (Fig. 5, upper panel). In the majority of infected cells, however, disassembly of actin was observed and stress fibers were undetectable or their numbers were significantly reduced (Fig. 5A, lower panel). A mean of 67 and 69% of cells infected with either the parental BAC20 or the $20U_S3$* virus, respectively, exhibited a disassembly of the actin cytoskeleton (Fig. 5B). In cells infected with the U_S3-negative virus, again both phenotypes of the actin cytoskeleton, i.e., the presence of intact stress fibers and disassembly of the actin cytoskeleton, were observed. In contrast to the observation with parental BAC20 or the revertant $20U_S3$* virus, however, infected cells with intact actin stress fibers were as frequent (49%) as those exhibiting actin disassembly (Fig. 5B). An analysis of variance revealed that the differences in the number of infected cells with intact actin stress fibers between $20\Delta U_S3$ and the parental or revertant virus were statistically significantly different ($P < 0.0382$).

To analyze the potential role of pU_S3 in actin disassembly in more detail and to more reliably quantify pU_S3-mediated actin stress fiber breakdown, expression plasmid pcU_S3* or gB-expressing control plasmid pcMgB was transfected into CEC. After transfection, the percentages of actin stress fiber-containing cells were determined at 24 and 48 h after transfection. Cells were fixed and analyzed by IIF using anti-FLAG MAb M2 or the gB-specific MAb 2K11. To visualize actin, cells were stained with AlexaFluor 488-phalloidin. Following transfection, disassembly of the actin cytoskeleton could clearly be observed in a mean of 74% of pU_S3*-expressing cells at the 24-h time point (Fig. 6), while gB-expressing cells showed almost no (6%) disassembly of the actin cytoskeleton. At the 48-h time point, however, the actin cytoskeleton had recovered in pU_S3*-expressing cells and stress fiber organization was intact in the vast majority of transfected cells (96%), as revealed by the AlexaFluor 488-phalloidin staining of actin fibers. At the later time point, no difference in the number of actin stress fiber-containing cells between U_S3*- or gB-expressing cells was observed (Fig. 6). The reduction in numbers of

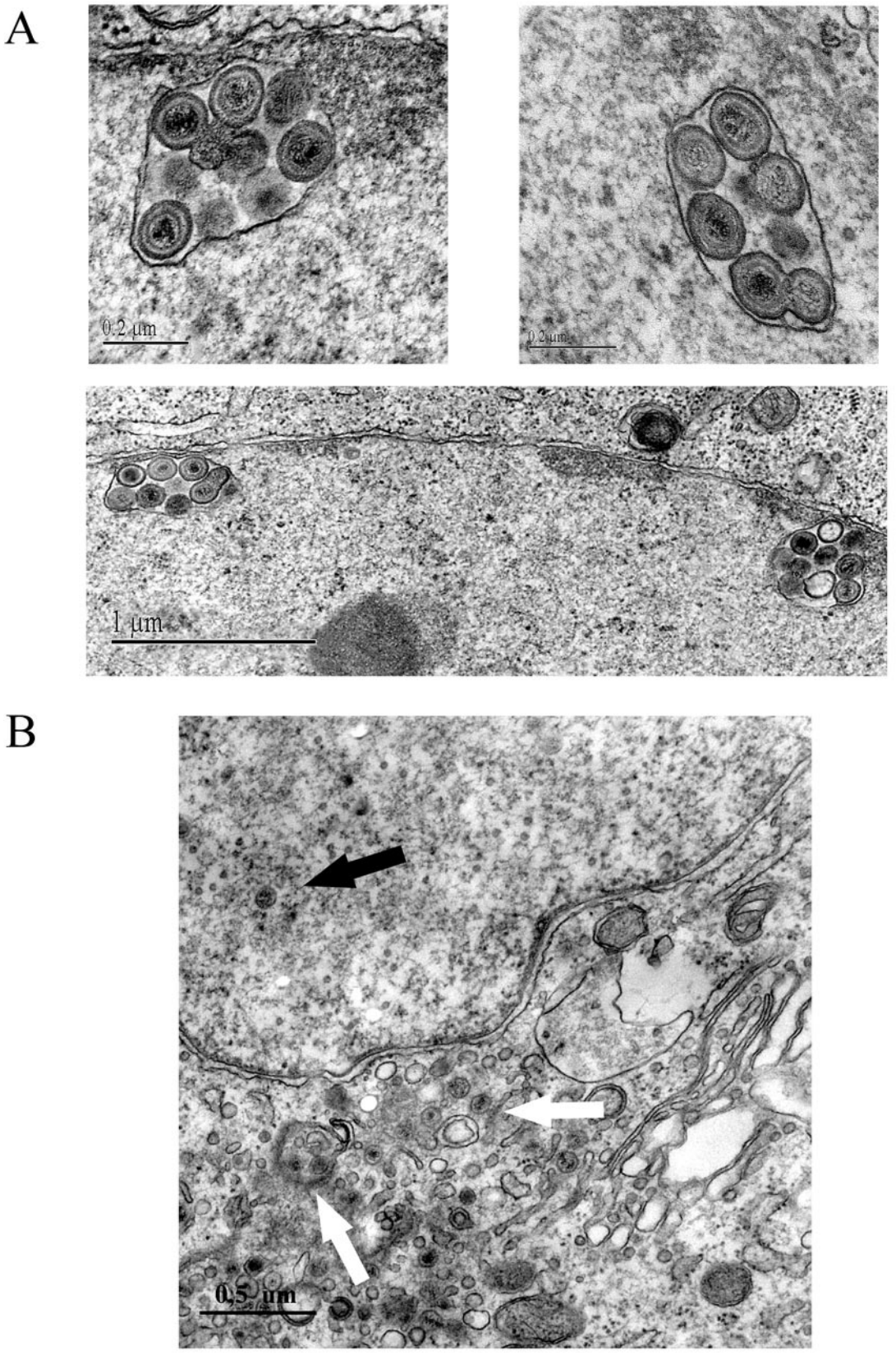

FIG. 4. Electron microscopy of $20\Delta U_S3$- or $20U_S3$*-infected CEC. Cells were infected with recombinant virus and fixed 3 days p.i. (A) Electron microscopic examination of the $20\Delta U_S3$ revealed an accumulation of enveloped virions in the perinuclear space in characteristic protrusions. (B) In cells infected with parental BAC20 (data not shown) or the $20U_S3$* revertant virus, all stages of virion morphogenesis were detectable, without any accumulation of primarily enveloped virions in the perinuclear space. A newly synthesized A-type capsid in the nucleus is marked with a black arrow, while naked nucleocapsids and mature viruses in transport vesicles in the cytoplasm are marked with white arrows. Note that no extracellular virus is released from $20U_S3$*- or $20\Delta U_S3$-infected cells.

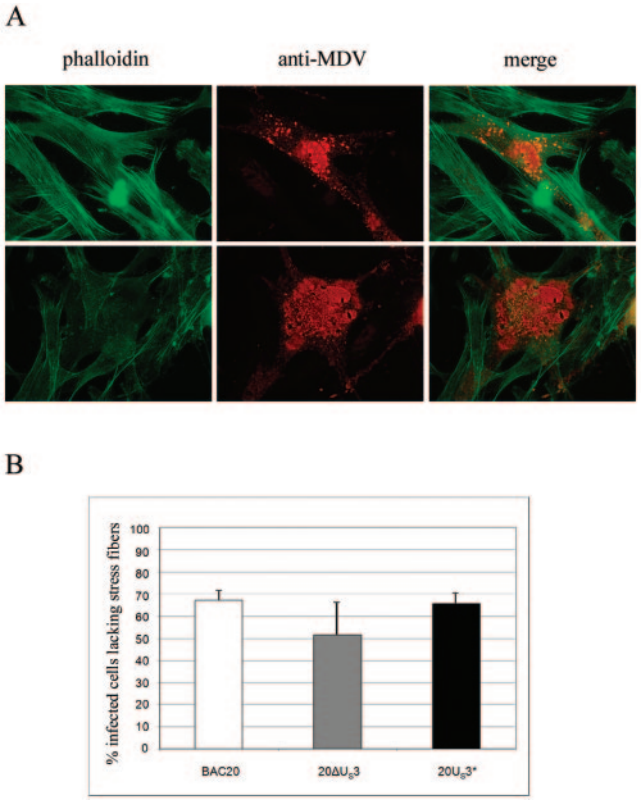

FIG. 5. (A) Disassembly of actin stress fibers in CEC infected with BAC20 at 48 h p.i. Cells were fixed with 90% acetone at 48 h after infection. MDV proteins were detected with polyclonal convalescent-phase serum that was visualized using an Alexa 568-conjugated anti-chicken IgG as the secondary antibody (red). Actin was visualized with phalloidin-Alexa 488 (green). Cells were finally inspected using a Zeiss Axiovert fluorescence microscope, and pictures were taken with a 40× objective before processing with Adobe Photoshop. (B) Percentage of infected cells with intact and depolymerized actin stress fibers. A total of 300 infected cells in three independent experiments were inspected.

cells exhibiting stress fiber disassembly at 48 h after pU_S3^* transfection did not appear to be caused by a destruction of these cells or their detachment from the solid support, because absolute counts of FLAG-positive cells slightly increased from the 24-h time point (total mean of counted cells, 216) to the 48-h time point (total mean of counted cells, 227). In addition, no gross morphological changes like cell rounding were detectable at either the earlier or later time point (Fig. 6A). We concluded from the experiments on the structure of the actin cytoskeleton in MDV-infected and pU_S3^*-transfected cells that MDV infection causes a reorganization of the actin cytoskeleton, but that this reorganization was transient and only partially mediated by pU_S3.

Polymerization of actin is important for cell-to-cell spread of MDV. To investigate the role of actin and microtubule dynamics in MDV infection, more specifically in viral cell-to-cell spread, BAC20-transfected cells were treated with various concentrations of cytochalasin D, a drug that prevents the repolymerization of G-actin (14), or nocodazole, which depolymerizes microtubules (8). In pilot experiments, toxic concentrations of cytochalasin D (10 μM) and nocodazole (75 μM) for CEC were determined. BAC20-transfected cells were then incubated for 5 days in the presence of 5, 0.5, or 0.05 μM cytochalasin D or 50, 5, or 0.5 μM nocodazole. These concentrations of cytochalasin D and nocodazole were shown to result in a dose-dependent disassembly of either F-actin or microtubules, respectively (Fig. 7A). In contrast, the concentrations of cytochalasin D or nocodazole used had no destabilizing effect on microtubule organization or the actin cytoskeleton in CEC, respectively (Fig. 7A).

At day 5 after transfection of the infectious virus DNA, cells were fixed and single infected cells and plaques were identified by IIF using anti-VP5 MAb 3F19 at a 1:100 dilution. Treat-

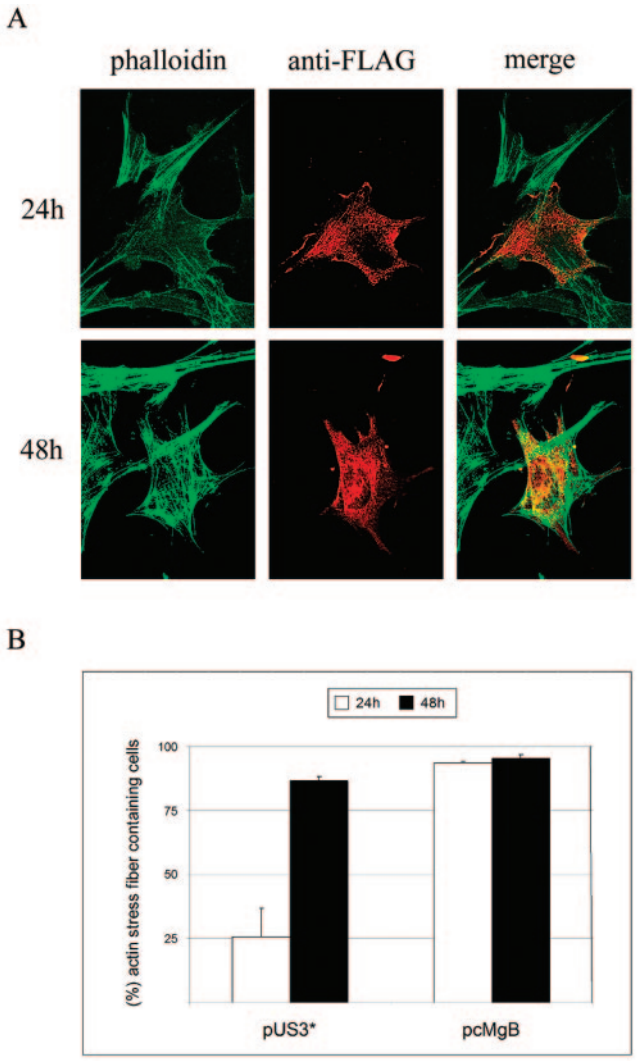

FIG. 6. (A) Subcellular localization of pU_S3^* in CEC transfected with expression plasmid pcU_S3^*. Cells were fixed at the given time points with 90% acetone, and FLAG-tagged U_S3 (red) was detected using the anti-FLAG M2 antibody and Alexa 568-conjugated anti-mouse IgG as the secondary antibody. Actin (green) was stained with phalloidin-Alexa 488. Red and green fluorescence signals were recorded separately by using appropriate filters with a confocal microscope (Olympus). Overlay of the pU_S3 and actin fluorescent signals is shown in the merge. (B) Percentages of pU_S3^*- and pcMgB-transfected cells with intact actin stress fibers (100 cells were scored) at 24 and 48 h after transfection. Percentages represent means and standard deviations of three independent experiments.

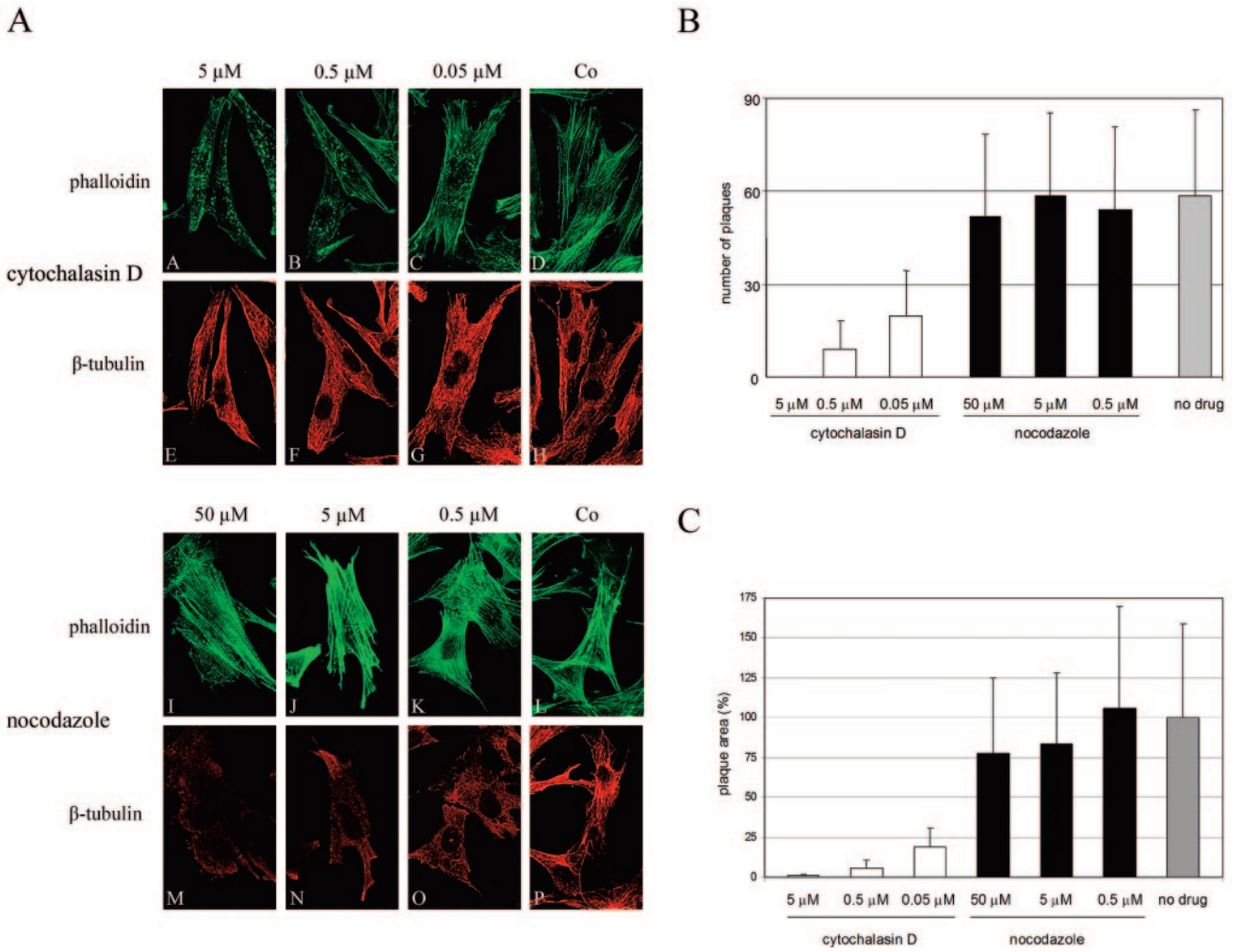

FIG. 7. (A) Effect of various concentrations of cytochalasin D (A to H) or nocodazole (I to P) on the actin cytoskeleton or microtubules in CEC, respectively. Cells were stained simultaneously with phalloidin-Alexa 488 to detect polymerized actin and with anti-α-tubulin–Alexa 546 to detect microtubules. Fluorescences were recorded individually by CLSM. A dose-dependent disassembly of actin stress fibers in the presence of cytochalasin D (A to C) and a gradual disassembly of microtubules with increasing concentrations of nocodazole (I to K) were observed. Note the presence of the microtubules in cytochalasin D-treated cells (E to G) and the intact actin stress fibers in cultures treated with nocodazole (I to K). Untreated control cells are in panels D, H, L, and P. (B) Number of plaques after transfection of BAC20 DNA in the presence or absence of cytochalasin D or nocodazole. CEC were transfected with 5 μg of BAC20 DNA, and the indicated concentrations of the drugs were added at 8 h after transfection. Media were changed twice daily to maintain drug concentrations. Five days after transfection, the number of plaques was determined after fixing the cells with 90% acetone and subsequent IIF using MAb 3F19, which recognizes the MDV major nucleocapsid protein VP5. Bars represent the number of plaques of four independent experiments performed in duplicate; standard deviations are given. (C) Plaque diameters after infection with BAC20 virus in the presence or absence of cytochalasin D or nocodazole. CEC were infected, and indicated concentrations of the drugs were added at 12 h after infection. Media were changed twice daily to maintain drug concentrations. Four days after infection, plaque sizes were determined after IIF staining with the MDV-specific chicken antiserum. Means and standard deviations of plaque areas of 100 plaques from two independent experiments are given.

ment of CEC with nocodazole did not have any inhibitory effect on the cell-to-cell spread capabilities of BAC20 virus, even when a concentration of 50 μM was used (Fig. 7B). This concentration of the drug not only resulted in complete disintegration of the microtubular network, but also in the beginning of cell rounding and partial disintegration of the monolayer (Fig. 7A).

In contrast to the inert effect of nocodazole on MDV cell-to-cell spread, a dose-dependent inhibition of MDV plaque formation was observed in the presence of cytochalasin D. Even concentrations of as low as 50 nM cytochalasin D had a significant inhibitory effect on virus spread, and plaque numbers were reduced by more than twofold (Fig. 7B). When the highest (5 μM) concentration of the drug was used, no plaque formation at all could be observed. This inhibitory effect on MDV cell-to-cell spread was not caused by an absence of virus reconstitution or production of late viral proteins in the presence of cytochalasin D, because single infected cells were readily detected by IIF and the numbers of single infected cells corresponded well to the number of plaques observed in the presence of nocodazole or when no drug was added after transfection of infectious BAC20 DNA.

The findings of a reduced number of virus plaques after cytochalasin D but not nocodazole treatment were corroborated by experiments that assessed the plaque areas after treatment of infected cells with the two drugs. Consistent with the findings described above, cytochalasin D concentrations of as low as 50 nM resulted in a significant decrease of plaque sizes, which was much more pronounced at higher cytochalasin D concentrations (Fig. 7C). In the case of a cytochalasin D concentration of 5 μM, almost no plaque formation was visible and mostly single infected cells were observed. In contrast, even in the presence of 50 mM nocodazole, which resulted in the complete absence of any microtubules and rounding of a substantive number of cells, mean plaque areas still reached 78% of those in the absence of any drug. At the lowest nocodazole concentrations of 0.5 μM, no negative influence on plaque formation was observed and mean plaque areas even appeared bigger than in BAC20-infected cells with no drug treatment (Fig. 7C). From these experiments we concluded that polymerizing actin plays an important role in MDV cell-to-cell spread, while an intact microtubular network appears to be dispensable for virus spread in cultured cells.

DISCUSSION

The U_S3-encoded protein kinases of alphaherpesviruses, more specifically those of HSV-1 and PRV, have been shown to be important players in the de-envelopment that primarily enveloped virions undergo by fusing with the outer leaflet of the nuclear membrane. This important step in virion morphogenesis results in the presence of naked nucleocapsids in the cytoplasm of infected cells. Although nonessential for virus growth in vitro, the deletion of U_S3 in HSV-1, PRV, and bovine herpesvirus type 1 results in reduced growth rates of mutant viruses (17, 35, 41), and the results reported here on the defect in efficient virus replication of an MDV U_S3 mutant are in good agreement with previous observations reported for related virus systems.

Our findings, however, are in contradiction to those reported by Sakaguchi et al. (36), who described an MDV U_S3 deletion mutant that did not show any growth defects. Those authors constructed an MDV strain K-544 mutant that expressed β-galactosidase instead of pU_S3. One possible explanation for the differing results is that the action of pU_S3 may be strain specific. An alternative explanation is that the U_S3-negative virus described previously was constructed by conventional marker rescue and plaque purified over 10 passages in eukaryotic cells. During plaque purification, spontaneous and compensatory mutations in other ORFs might have arisen that could explain the virtually identical growth properties of the U_S3 mutant and the parental virus. This latter interpretation is supported by the observation that the growth defect of $20\Delta U_S3$ was only noticeable for a few passages in CEC; afterwards, plaque sizes were restored to near-wild-type levels. This phenomenon of a restoration of the growth deficits in the absence of pU_S3 after only a few rounds of replication in CEC and the identification of the compensatory mutation(s) are currently being addressed in our laboratory.

We view it as unlikely that the U_S2 product, which is absent in BAC20 and derivatives thereof (39), cooperates with pU_S3 in the early stages of MDV morphogenesis, because the U_S2 homologues in equine herpesvirus type 1 and PRV seem to function very late in virus assembly and egress (2, 24). In addition, pU_S3 was shown to be involved in two mechanisms that may contribute to the observed phenotype of inefficient cell-to-cell spread of a U_S3-negative MDV mutant. One of the actions of MDV pU_S3, which is similar to those of the HSV-1 and PRV U_S3 proteins, is its involvement in efficient release of primarily enveloped viruses from the ER, which leads to a reduced number of cytoplasmic virions and may consequently result in a less-efficient infection of neighboring cells because fewer infectious particles may finally reach the plasma membrane.

A second function of pU_S3 that may be important in a later stage of cell-to-cell spread and one that was first observed in PRV is its ability to break down actin stress fibers in infected cells (44). We asked the question whether the MDV unique-short protein kinase would also be exerting an action on the actin cytoskeleton, the disassembly of which can be observed in infected cells at early and late times p.i. In cultures infected with the parental BAC20 or the revertant $20U_S3^*$ virus, the majority of cells lacked an intact actin cytoskeleton. This observation—although to a lesser extent—was also made with the $20\Delta U_S3$ mutant virus. Quantification of the number of cells with depolymerized actin after infection, however, proved to be extremely difficult, because the highly cell-associated nature of MDV requires a coseeding of infected with uninfected cells and synchronous high-multiplicity infections are impossible. However, there was a significant difference of 15% between the number of infected cells exhibiting intact actin stress fibers in CEC infected with $20\Delta U_S3$ compared to those infected with parental or revertant virus. Moreover, in cells transiently expressing U_S3^* under the control of the human cytomegalovirus immediate-early promoter, we observed actin depolymerization in the first 24 h after transfection. Surprisingly, at later times after transfection U_S3-expressing cells had intact actin stress fibers. These experiments demonstrated that pU_S3 is clearly involved in actin depolymerization but indicated that (i) pU_S3 is not absolutely necessary for actin disassembly in MDV-infected cells, especially at later times p.i., (ii) the action of pU_S3 on polymerized actin is transient, and (iii) sustained depolymerization requires other MDV infected cell proteins. The transient nature of pU_S3-mediated actin stress fiber breakdown in transfected cells was unexpected. A possible explanation may be that immunological detection of the kinase is still possible at later time points after transfection, but that pU_S3 exhibits decreased functional stability when transiently expressed in the absence of other viral proteins. Mechanistically, MDV-induced actin depolymerization may be harnessed to facilitate spread from an infected to a neighboring uninfected cell by exploiting directional repolymerization of the monomeric G-actin for intra- and intercellular movement, possibly similar to the mechanism used by vaccinia virus (3). MDV is strictly cell associated and does not produce free virus; rather, it only uses direct cell-cell spread for virus replication and growth. In this context it is interesting that we were also able to demonstrate a massive reduction in the ability of MDV to form plaques in the presence of cytochalasin D, a drug that prevents the repolymerization of monomeric actin, while nocodazole, which disintegrates microtubules, did not have a strong effect on MDV plaque formation. These results obtained after both

transfection of BAC20 DNA and after infection strongly indicated that MDV cell-to-cell spread is dependent on the ability of monomeric actin to polymerize but does not require an intact microtubular network. Further experiments are targeted towards a more detailed analysis of this putative interaction between MDV and the cytoskeleton and its functional implications.

A further known function of pU_S3 homologues is phosphorylation of both viral and cellular proteins. In fact, preliminary data obtained from Western blot studies using cloned MDV U_S3 and the available U_S3 mutant viruses suggest that the MDV-specific early viral protein pp38 is one target of the unique-short-encoded serine/threonine kinase. MDV pp38, encoded by R-LORF14a (MDV073), has been shown to be phosphorylated at serine residues and was originally proposed to be directly involved in tumor development (4). Recent evidence strongly suggests, however, an involvement of pp38 in the early lytic stages of virus infection, which ultimately results in a lower incidence of latently infected cells and tumors. Presently, we do not know whether the prototype target of phosphorylation by pU_S3, the U_L34 product, is phosphorylated by the MDV serine/threonine protein kinase. HSV-1 pU_L34 was the first viral protein that was shown to stay unphosphorylated in the absence of pU_S3 (29, 30). As stated above, the U_L34 gene encodes a type II transmembrane protein that is essential for primary envelopment of nucleocapsids and primarily localizes to the nuclear envelope of infected cells (30, 31). Interestingly, phosphorylation of the PRV U_L34 homologous protein was not altered in the absence of the unique-short protein kinase and can probably also be phosphorylated by cellular kinases (17). Similarly, absence of pU_S3 and, consequently, lack of pU_S3-mediated phosphorylation of the HSV-1 U_L34 product did not result in replication-deficient virus, unlike viruses in which pU_L34 was deleted (31, 35). Currently, we are conducting experiments that address the kinase activity of MDV pU_S3, and we are concentrating on the putative phosphorylation of pp38 and pU_L34 by the unique-short protein kinase. Recent evidence obtained for the interaction between HSV-1 pU_S3 and pU_L34 suggests that the kinase activity of pU_S3 is required for efficient de-envelopment, but that the kinase targets an infected cell protein other than pU_L34 (35). Our studies address the question of whether the accumulation of enveloped virions at the nuclear rim in the absence of MDV pU_S3 is caused by structural deficits in the absence of a tegument protein or by the absence of phosphorylation of target viral or cellular proteins. These studies will involve a comparison of the functionality of wild-type and mutant MDV pU_S3 in which the kinase domain is altered.

ACKNOWLEDGMENTS

We thank Neal Copeland (Center for Cancer Research, National Cancer Institute, Frederick, Md.) for the EL250 bacteria, Barry Wanner (Purdue University, West Lafayette, Ind.) for plasmid pKD13, and Jean-Francois Vautherot (INRA, Tours, France) for providing MAbs 2K11, 3F19, and L13.

REFERENCES

1. **Baines, J. D., and B. Roizman.** 1992. The U_L11 gene of herpes simplex virus 1 encodes a function that facilitates nucleocapsid envelopment and egress from cells. J. Virol. **66:**5168–5174.
2. **Clase, A. C., M. G. Lyman, T. del Rio, J. A. Randall, C. M. Calton, L. W. Enquist, and B. W. Banfield.** 2003. The pseudorabies virus U_S2 protein, a virion tegument component, is prenylated in infected cells. J. Virol. **77:** 12285–12298.
3. **Cudmore, S., P. Cossart, G. Griffiths, and M. Way.** 1995. Actin-based motility of vaccinia virus. Nature **378:**636–638.
4. **Cui, Z. Z., L. F. Lee, J. L. Liu, and H. J. Kung.** 1991. Structural-analysis and transcriptional mapping of the Marek's disease virus gene encoding pp38, an antigen associated with transformed cells. J. Virol. **65:**6509–6515.
5. **Datsenko, K. A., and B. L. Wanner.** 2000. One-step inactivation of chromosomal genes in Escherichia coli K-12 using PCR products. Proc. Natl. Acad. Sci. USA **97:**6640–6645.
6. **Davison, A.** 2002. Comments on the phylogenetics and evolution of herpesviruses and other large DNA viruses. Virus Res. **82:**127–132.
7. **Davison, A. J.** 2002. Evolution of the herpesviruses. Vet. Microbiol. **86:**69–88.
8. **De Brabander, M. J., R. M. Van de Veire, F. E. Aerts, M. Borgers, and P. A. Janssen.** 1976. The effects of methyl (5-(2-thienylcarbonyl)-1H-benzimidazol-2-yl) carbamate, (R 17934; NSC 238159), a new synthetic antitumoral drug interfering with microtubules, on mammalian cells cultured in vitro. Cancer Res. **36:**905–916.
9. **Dorange, F., S. El Mehdaoui, C. Pichon, P. Coursaget, and J. F. Vautherot.** 2000. Marek's disease virus (MDV) homologues of herpes simplex virus type 1 UL49 (VP22) and UL48 (VP16) genes: high-level expression and characterization of MDV-1 VP22 and VP16. J. Gen. Virol. **81:**2219–2230.
10. **Dorange, F., B. K. Tischer, J. F. Vautherot, and N. Osterrieder.** 2002. Characterization of Marek's disease virus serotype 1 (MDV-1) deletion mutants that lack UL46 to UL49 genes: MDV-1 UL49, encoding VP22, is indispensable for virus growth. J. Virol. **76:**1959–1970.
11. **Foster, T. P., and K. G. Kousoulas.** 1999. Genetic analysis of the role of herpes simplex virus type 1 glycoprotein K in infectious virus production and egress. J. Virol. **73:**8457–8468.
12. **Foster, T. P., G. V. Rybachuk, X. Alvarez, O. Borkhsenious, and K. G. Kousoulas.** 2003. Overexpression of gK in gK-transformed cells collapses the Golgi apparatus into the endoplasmic reticulum inhibiting virion egress, glycoprotein transport, and virus-induced cell fusion. Virology **317:**237–252.
13. **Foster, T. P., G. V. Rybachuk, and K. G. Kousoulas.** 2001. Glycoprotein K specified by herpes simplex virus type 1 is expressed on virions as a Golgi complex-dependent glycosylated species and functions in virion entry. J. Virol. **75:**12431–12438.
14. **Goddette, D. W., and C. Frieden.** 1986. Actin polymerization. The mechanism of action of cytochalasin D. J. Biol. Chem. **261:**15974–15980.
15. **Granzow, H., B. G. Klupp, W. Fuchs, J. Veits, N. Osterrieder, and T. C. Mettenleiter.** 2001. Egress of alphaherpesviruses: comparative ultrastructural study. J. Virol. **75:**3675–3684.
16. **Jayachandra, S., A. Baghian, and K. G. Kousoulas.** 1997. Herpes simplex virus type 1 glycoprotein K is not essential for infectious virus production in actively replicating cells but is required for efficient envelopment and translocation of infectious virions from the cytoplasm to the extracellular space. J. Virol. **71:**5012–5024.
17. **Klupp, B. G., H. Granzow, and T. C. Mettenleiter.** 2001. Effect of the pseudorabies virus US3 protein on nuclear membrane localization of the UL34 protein and virus egress from the nucleus. J. Gen. Virol. **82:**2363–2371.
18. **Kopp, M., H. Granzow, W. Fuchs, B. G. Klupp, E. Mundt, A. Karger, and T. C. Mettenleiter.** 2003. The pseudorabies virus UL11 protein is a virion component involved in secondary envelopment in the cytoplasm. J. Virol. **77:**5339–5351.
19. **Kyhse-Andersen, J.** 1984. Electroblotting of multiple gels: a simple apparatus without buffer tank for rapid transfer of proteins from polyacrylamide to nitrocellulose. J. Biochem. Biophys. Methods **10:**203–209.
20. **Lee, E. C., D. Yu, V. de Martinez, L. Tessarollo, D. A. Swing, Court, D. L., N. A. Jenkins, and N. G. Copeland.** 2001. A highly efficient Escherichia coli-based chromosome engineering system adapted for recombinogenic targeting and subcloning of BAC DNA. Genomics **73:**56–65.
21. **Leopardi, R., C. Van Sant, and B. Roizman.** 1997. The herpes simplex virus 1 protein kinase US3 is required for protection from apoptosis induced by the virus. Proc. Natl. Acad. Sci. USA **94:**7891–7896.
22. **Loomis, J. S., J. B. Bowzard, R. J. Courtney, and J. W. Wills.** 2001. Intracellular trafficking of the UL11 tegument protein of herpes simplex virus type 1. J. Virol. **75:**12209–12219.
23. **Loomis, J. S., R. J. Courtney, and J. W. Wills.** 2003. Binding partners for the U_L11 tegument protein of herpes simplex virus type 1. J. Virol. **77:**11417–11424.
24. **Meindl, A., and N. Osterrieder.** 1999. The equine herpesvirus 1 U_S2 homolog encodes a nonessential membrane-associated virion component. J. Virol. **73:**3430–3437.
25. **Muyrers, J. P., Y. Zhang, G. Testa, and A. F. Stewart.** 1999. Rapid modification of bacterial artificial chromosomes by ET-recombination. Nucleic Acids Res. **27:**1555–1557.
26. **Ogg, P. D., P. J. McDonell, B. J. Ryckman, C. M. Knudson, and R. J. Roller.** 2004. The HSV-1 Us3 protein kinase is sufficient to block apoptosis induced by overexpression of a variety of Bcl-2 family members. Virology **319:**212–224.
27. **Osterrieder, N., A. Neubauer, C. Brandmuller, O. R. Kaaden, and D. J.**

O'Callaghan. 1998. The equine herpesvirus 1 IR6 protein that colocalizes with nuclear lamins is involved in nucleocapsid egress and migrates from cell to cell independently of virus infection. J. Virol. **72:**9806–9817.
28. **Osterrieder, N., and J. F. Vautherot.** 2004. The genome content of Marek's disease-like viruses, p. 17-31. *In* F. Davison and V. Nair (ed.), Marek's Disease—an evolving problem. Elsevier, London, England.
29. **Purves, F. C., R. M. Longnecker, D. P. Leader, and B. Roizman.** 1987. Herpes simplex virus 1 protein kinase is encoded by open reading frame US3 which is not essential for virus growth in cell culture. J. Virol. **61:**2896–2901.
30. **Purves, F. C., D. Spector, and B. Roizman.** 1991. The herpes simplex virus 1 protein kinase encoded by the US3 gene mediates posttranslational modification of the phosphoprotein encoded by the UL34 gene. J. Virol. **65:**5757–5764.
31. **Reynolds, A. E., B. J. Ryckman, J. D. Baines, Y. Zhou, L. Liang, and R. J. Roller.** 2001. U_L31 and U_L34 proteins of herpes simplex virus type 1 form a complex that accumulates at the nuclear rim and is required for envelopment of nucleocapsids. J. Virol. **75:**8803–8817.
32. **Reynolds, A. E., E. G. Wills, R. J. Roller, B. J. Ryckman, and J. D. Baines.** 2002. Ultrastructural localization of the herpes simplex virus type 1 UL31, UL34, and US3 proteins suggests specific roles in primary envelopment and egress of nucleocapsids. J. Virol. **76:**8939–8952.
33. **Rispens, B. H., H. van Vloten, N. Mastenbroek, J. L. Maas, and K. A. Schat.** 1972. Control of Marek's disease in the Netherlands. II. Field trials on vaccination with an avirulent strain (CVI 988) of Marek's disease virus. Avian Dis. **16:**126–138.
34. **Roizman, B., and A. E. Sears.** 1996. Herpes simplex viruses and their replication, p. 2231-2295. *In* B. N. Fields, D. M. Knipe, and P. M. Howley (ed.), Fields virology. Lippincott-Raven Press, Phliadelphia, Pa.
35. **Ryckman, B. J., and R. J. Roller.** 2004. Herpes simplex virus type 1 primary envelopment: UL34 protein modification and the US3-UL34 catalytic relationship. J. Virol. **78:**399–412.
36. **Sakaguchi, M., T. Urakawa, Y. Hirayama, N. Miki, M. Yamamoto, G. S. Zhu, and K. Hirai.** 1993. Marek's disease virus protein kinase gene identified within the short unique region of the viral genome is not essential for viral replication in cell culture and vaccine-induced immunity in chickens. Virology **195:**140–148.
37. **Sambrook, J., D. F. Fritsch, and T. Maniatis.** 1989. Molecular cloning: a laboratory manual, 2nd ed. Cold Spring Harbor Laboratory Press, Cold Spring Harbor, N.Y.
38. **Schimmer, C., and A. Neubauer.** 2003. The equine herpesvirus 1 UL11 gene product localizes to the trans-Golgi network and is involved in cell-to-cell spread. Virology **308:**23–36.
39. **Schumacher, D., B. K. Tischer, W. Fuchs, and N. Osterrieder.** 2000. Reconstitution of Marek's disease virus serotype 1 (MDV-1) from DNA cloned as a bacterial artificial chromosome and characterization of a glycoprotein B-negative MDV-1 mutant. J. Virol. **74:**11088–11098.
40. **Schumacher, D., B. K. Tischer, S. M. Reddy, and N. Osterrieder.** 2001. Glycoproteins E and I of Marek's disease virus serotype 1 are essential for virus growth in cultured cells. J. Virol. **75:**11307–11318.
41. **Takashima, Y., H. Tamura, X. Xuan, and H. Otsuka.** 1999. Identification of the US3 gene product of BHV-1 as a protein kinase and characterization of BHV-1 mutants of the US3 gene. Virus Res. **59:**23–34.
42. **Tischer, B. K., D. Schumacher, M. Messerle, M. Wagner, and N. Osterrieder.** 2002. The products of the UL10 (gM) and the UL49.5 genes of Marek's disease virus serotype 1 are essential for virus growth in cultured cells. J. Gen. Virol. **83:**997–1003.
43. **Tulman, E. R., C. L. Afonso, Z. Lu, L. Zsak, D. L. Rock, and G. F. Kutish.** 2000. The genome of a very virulent Marek's disease virus. J. Virol. **74:**7980–7988.
44. **Van Minnebruggen, G., H. W. Favoreel, L. Jacobs, and H. J. Nauwynck.** 2003. Pseudorabies virus US3 protein kinase mediates actin stress fiber breakdown. J. Virol. **77:**9074–9080.
45. **Witter, R. L.** 2001. Protective efficacy of Marek's disease. Vaccines **255:**57–90.
46. **Witter, R. L., L. F. Lee, and A. M. Fadly.** 1995. Characteristics of CVI988/Rispens and R2/23, two prototype vaccine strains of serotype 1 Marek's disease virus. Avian Dis. **39:**269–284.
47. **Ye, G. J., and B. Roizman.** 2000. The essential protein encoded by the UL31 gene of herpes simplex virus 1 depends for its stability on the presence of UL34 protein. Proc. Natl. Acad. Sci. USA **97:**11002–11007.